QUASI-STATIC MECHANICAL BEHAVIOUR OF TI-6AL-4V ALLOY AT ROOM TEMPERATURE

V. TUNINETTI[*], G. GILLES[*], O. MILIS[*], I. NEIRA[*], A.M. HABRAKEN[†*]

[*] ArGEnCo, Division MS^{2}F
University of Liège
Chemin des Chevreuils 1, 4000 Liège, Belgium
e-mail: V.Tuinetti@ulg.ac.be, www.argenco.ulg.ac.be/ms2f_EN.php

[†] Research Director of the National Fund for Scientific Research, Belgium

Keywords: Ti-6Al-4V (TA6V), Material characterization, Plastic anisotropy, strength differential effect (SD), CPB06 yield locus.

Abstract. In order to determine the mechanical behavior of a bulk TA6V alloy, a set of mechanical tests such as shear, compression, tensile monotonic tests, and tensile tests on notched samples are performed. The material is tested at constant strain rate. Full-field optical technique for displacement measurements and strain computation are used for all the experiments. Plastic anisotropy and tension–compression asymmetry are observed. The CPB06 [1] yield criterion adapted for hexagonal close packed (hcp) material is identified. The sensitivity of the material parameters on the identification method as well as the efficiency of the model to predict forces and displacement field are discussed. Validation is done by using Finite Element method (FEM) simulations and 3D Digital Image Correlation (3D-DIC) measurements on specimens with multi-axial stress and strain fields subjected to large deformation.

1 INTRODUCTION

TA6V is one of the most frequently used titanium alloy in aerospace applications such as turbine blades, due to their high strength to weight ratio, ductility, ability to withstand high temperatures and to resist corrosion. Several studies have been done in order to understand the mechanical behavior of TA6V. This alloy exhibits a pronounced anisotropy and a strength asymmetry between tension and compression [2, 3, 4, 5]. In addition, flow stress of TA6V is strongly dependent on both temperature and strain rate [6, 7, 4]. In order to predict the quasi-static mechanical behaviour of TA6V at room temperature (RT), the well-known macroscopic orthotropic yield criterion CPB06 proposed by Cazacu et al. [1,8] was identified by using a set of material monotonic tests performed on TA6V at room temperature and at low strain rate of 10^{-3} s^{-1}. The sensitivity of the material parameters on the identification method as well as the efficiency of the model to predict forces and displacement field are discussed. Then, a validation of the model was done in specimens with multi-axial stress strain fields and large deformations.

2 EXPERIMENTAL PROCEDURE

Compression, tension, shear and plane strain specimens were machined from the initial bulk TA6V alloy with the dimension shown in Fig. 1(a). Both tensile and compression tests were performed in three orthogonal directions: Longitudinal (LD), Transverse (TD) and Short Transverse (ST). Shear and plane strain tests were performed in ST-LD direction.

Due to the high strain rate and temperature sensitivity of this hcp alloy in quasi-static loading, the tests were performed at room temperature and the strain rate targeted was at a constant value of 10^{-3} s^{-1}. These tests were carried out in the University of Liège, except tensile tests in TD and ST directions that were performed in the "Université Catholique de Louvain".

2.1 Material

The bulk TA6V titanium alloy tested has a chemical composition shown in table 1. Optical microscopy showed that the material has slightly elliptic grain and the mean grain size is 12 µm in ST-LD plane and 9µm in ST-TD plane. The α-phase represents 94% of the volume. The initial texture of the material was determined by X-ray diffraction (XRD). It is shown in Fig. 1b that this alloy is low textured material.

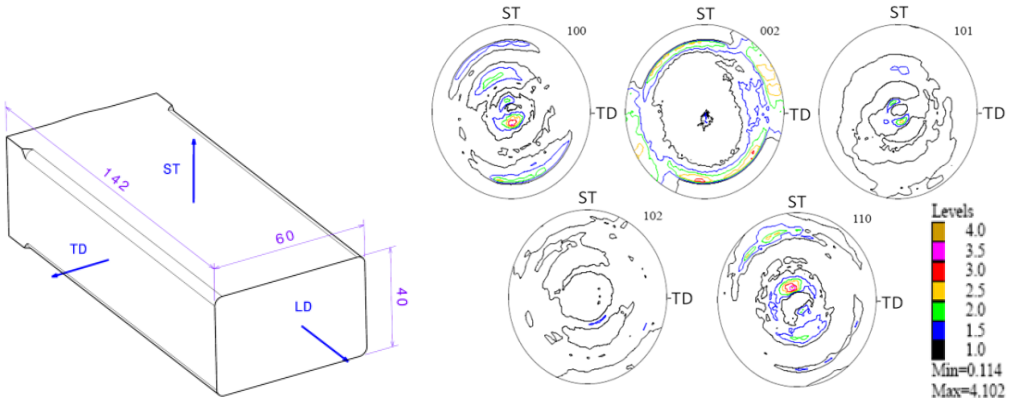

Figure 1: (a) Material direction of bulk TA6V. (b) Initial texture of TA6V.

Table 1: Chemical composition of the TA6V alloy investigated (wt%)

Al	V	Fe	N	O	C	Ti
6.1	4.0	0.3	0.05	0.20	0.08	Bal.

2.2 Compression tests

Specimens were machined by wire electron discharge machining (EDM) with dimensions shown in Fig. 2. The experiments were performed in three orthogonal material directions: LD, TD and ST. A servo hydraulic axial testing machine was controlled in order to obtain constant strain rate of 10^{-3} s^{-1}. Three 3D optical measurement systems (6 CCD cameras) were used and strain/displacement fields were measured for characterization and validation purposes (Fig.2). Stress-strain curves were computed by the method proposed by [9]. Cross-section of the

specimen is obtained by fitting an ellipse with the experimental data. By using the load measured by the load cell, the true stress is computed. True strain is obtained by averaging the axial strain measured on the surface of the horizontal symmetric plane of the sample.

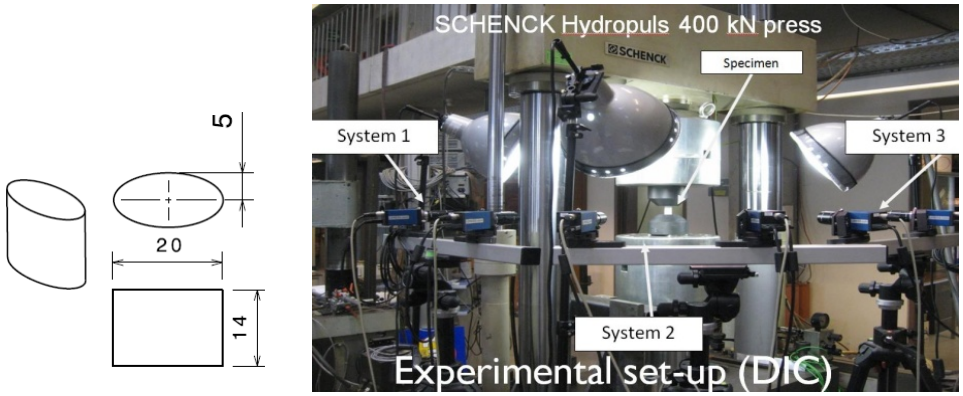

Figure 2: Compression test set-up and dimensions of the sample.

2.3 Tension tests

Axisymmetric specimens of 6mm in diameter for LD direction were tested at constant strain rate of 10^{-3} s^{-1} by an electro-mechanic Press ZWICK 100 kN and three 3D-DIC systems were used for strain/displacement measurements. By using the cross-section evolution of the tensile samples during the tests measured by DIC, a "Lankford" parameter similar to what is used for sheet was computed. It is defined as the ratio of the strain rate in the TD direction and in the ST direction: $R_{LD} = \dot{\varepsilon}_{TD} / \dot{\varepsilon}_{ST}$ where $\dot{\varepsilon}_{TD} = \ln(b/r)/t$ and $\dot{\varepsilon}_{ST} = \ln(a/r)/t$. r is the initial radius of the sample and *a, b* the major and minor axis lengths of the elliptical actualized cross-section of the specimen. *t* is the time since test start.

For TD and ST directions, tensile tests on axisymmetric specimens of 4mm in diameter have been carried out on a Zwick universal testing machine equipped with a digital extensometer. The machine was piloted in order to keep constant cross-head speed. The stress strain curves obtained for average plastic strain rates of $7x10^{-4}$ s^{-1} in TD and $9x10^{-5}$ s^{-1} in ST were transformed into 10^{-3} s^{-1} by using Johnson-Cook's viscoplastic model. This was done with the purpose of identifying the anisotropic yield locus at the same strain rate (10^{-3} s^{-1}). The choice of JC model was done due to its advantage of few constants and its ability to model the observed material response as closely as models with many more constants [7, 10].

2.4 Shear and plane strain tests

The tests were carried out with the biaxial machine developed and validated in the University of Liège (Fig. 3) [11]. This machine uses a vertical (A1) and a horizontal (A2) actuators which enable the displacements of the grips (G). These actuators were controlled by a computer in displacement with constant speed in order to reach plastic strain rates between $1x10^{-3}$ and $2x10^{-3}$ s^{-1} and elastic strain rates from $1x10^{-4}$ to $4x10^{-4}$ s^{-1}. For strain/displacement measurements, two 3D-DIC systems were used. The true stress for plane strain test was computed with the method proposed by Flores et al. [12]. This new accurate computation method uses experimental data and includes the edge effect evolution as a function of plastic

strain. In case of shear tests, the edge effect is negligible and shear stress can be accurately computed by: $\tau=F/A_0$. F is the load and A_0 is the initial cross-section of the sample.

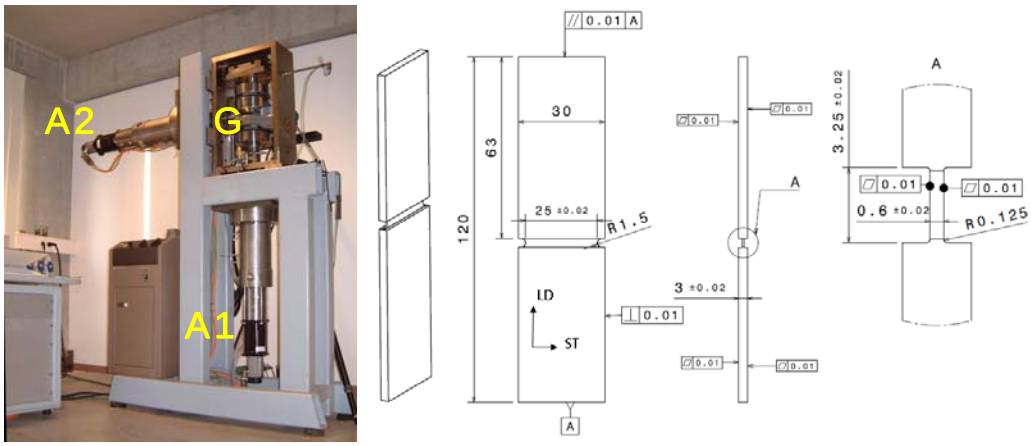

Figure 3: Sample of plane strain and shear tests.

2.5 Experimental Results

Three tests were performed for each monotonic test. The average curves obtained are presented in Fig. 4. The material response of TA6V demonstrates the strength asymmetry between tension and compression. Anisotropic yielding is found and is observed to be stronger in compression than in tension. "R value" in tension LD is computed and its value is $R_{LD} = \dot{\varepsilon}_{TD} / \dot{\varepsilon}_{ST} = 1.15$.

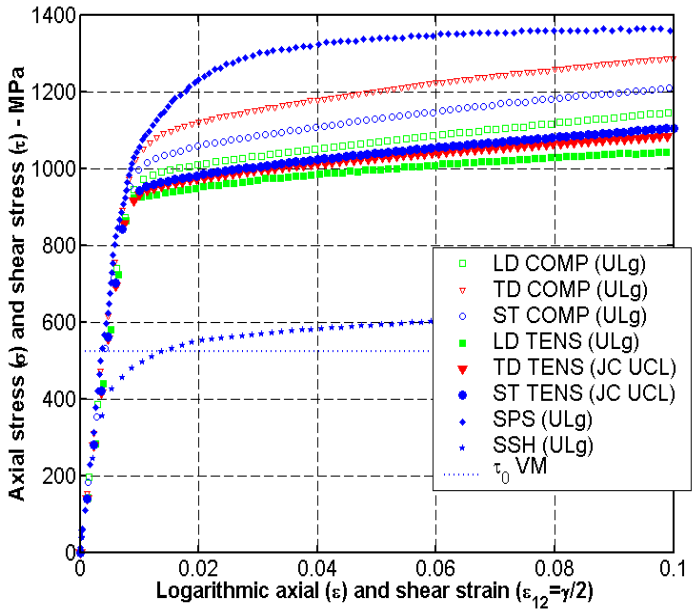

Figure 4: True stress strain curves for monotonic tensile and compression in three orthogonal material directions (LD, TD and ST), plane strain (SPS), and shear (SSH) at 10^{-3} s^{-1} and at RT.

Isotropic hardening is related to dislocation density and can be modeled by a simple homothetic increase of the yield locus. In this case, either Voce model or Swift model is fitted on tensile stress strain curve and applied. For the TA6V case, it is more complex. As seen in Fig 4, hardening rate is different in tension, compression and shear tests. And also, it varies with different loading directions. For this reason, in the next section a fitting of the yield loci at several plastic works considering the shape updating of the CPB06 criterion is chosen. Among other phenomena, the texture evolution and the effect of twinning can explain these macroscopic observations.

3 MODELING APPROACH

The well-known macroscopic orthotropic yield criterion CPB06 proposed by Cazacu et al. [1,8], is chosen, as it describes both the tension/compression asymmetry and the anisotropic behavior. Anisotropic hardening behavior is described by linear interpolation of CPB06 yield loci identified at several plastic work levels.

3.1 Anisotropic yield function

The CPB06 yield criterion proposed by Cazacu *et al.* (2006) is defined by:

$$F_1 = \left(|\Sigma_1| - k\Sigma_1\right)^a + \left(|\Sigma_2| - k\Sigma_2\right)^a + \left(|\Sigma_3| - k\Sigma_3\right)^a = \bar{\sigma}^a \tag{1}$$

$\Sigma_1, \Sigma_2, \Sigma_3$ are the principal values of the tensor Σ_{ij} defined by $\Sigma_{ij} = C_{ijkl} S_{kl}$ where C_{ijkl} is a fourth-order orthotropic tensor that accounts for the plastic anisotropy of the material. $\boldsymbol{S}$ is the deviator of the Cauchy stress tensor. k is a parameter which takes into account the strength differential effect (SD), a is the degree of homogeneity and $\bar{\sigma}$ is the equivalent stress associated with this criterion.

3.2 Hardening description

For monotonic loadings, the general practice is to assume isotropic hardening and using a representative hardening curve (in LD) as input for FE simulations. Isotropic hardening implies a proportional expansion of the surface, without any change in shape or position. Thus, for monotonic loading processes an isotropic hardening model is valid only if the material hardens at the same rate for every strain paths. However, as shown in Figure 4(a) and for hexagonal materials (see uniaxial stress-strain curves; Lou *et al.* (2007) [13]; Nixon *et al.* (2010), etc.) the rate of hardening depends on the loading direction and/or its orientation even for the simplest loading paths. A methodology that describes directional hardening of hexagonal materials has been proposed by Plunkett *et al.* (2006) [14] and used by Gilles et al. (2011) [3]. It consists in determining the anisotropy coefficients corresponding to several fixed levels of plastic work per unit volume $W_p^{(1)} < \ldots < W_p^{(j)} < \ldots < W_p^{(m)}$, $j = 1 \ldots m$, where $W_p^{(1)}$ corresponds to initial yielding and $W_p^{(m)}$ corresponds to the highest level of plastic work reached in all mechanical tests. Next, for each of the individual plastic work levels, $W_p^{(j)}$, $\bar{\sigma}$ is calculated using Eq. (1). Then, piece-wise linear interpolation is used in order to determine the yield surface corresponding to an intermediate level of plastic work.

3.3 Identification of parameters of CPB06 yield criterion

The anisotropy coefficients and SD parameters of CPB06 yield criterion are fitted on experimental yield stress ratios and r-ratios using the Simulated Annealing (SA) algorithm [14, 15, 16]. This is a global optimization method that distinguishes between different local optima. In this study, the error function to be minimized is defined as follows:

$$E = \sum_{i=1}^{r} \eta_i \left[\frac{\left(\sigma_D^T / \sigma_{LD}^T\right)_i^{\text{num}}}{\left(\sigma_D^T / \sigma_{LD}^T\right)_i^{\text{exp}}} - 1 \right]^2 + \sum_{j=1}^{s} \eta_j \left[\frac{\left(\sigma_D^C / \sigma_{LD}^T\right)_j^{\text{num}}}{\left(\sigma_D^C / \sigma_{LD}^T\right)_j^{\text{exp}}} - 1 \right]^2 + \sum_{k=1}^{t} \eta_k \left[\frac{\left(\sigma_D^{SPS} / \sigma_{LD}^T\right)_k^{\text{num}}}{\left(\sigma_D^{SPS} / \sigma_{LD}^T\right)_k^{\text{exp}}} - 1 \right]^2 + \dots + \sum_{l=1}^{u} \eta_l \left[\frac{\left(\sigma_D^{SSH} / \sigma_{LD}^T\right)_l^{\text{num}}}{\left(\sigma_D^{SSH} / \sigma_{LD}^T\right)_l^{\text{exp}}} - 1 \right]^2 + \sum_{m=1}^{v} \eta_m \left[\frac{r_m^{\text{num}}}{r_m^{\text{exp}}} - 1 \right]^2 \quad (2)$$

where *r, s, t, u* and *v* are respectively the number of tensile, compressive, plane strain, shear yield stresses, and available r-ratios. The superscript indicates whether the value is experimental (exp) or numerical (num). Parameters $\eta_{i,j,k,l,m}$ are eventually used to balance the weight of each term. This first identification step provided an initial set of parameter that was further adjusted. Inverse modelling of compression tests provide a second refined parameter set. This identification step fits the modelled response with the experimental axial strain distribution measured in the median cross-section of the specimen by 3D-DIC for LD, TD and ST directions. One-eighth of specimen model was used for the numerical simulation within the updated Lagrangian FE code Lagamine. Friction Coulomb coefficient was considered constant and its value $\Phi = 0.08$ was obtained by fitting the measured and predicted barreling. Finally, these two identification steps provide a material data set based on compression and tension tests in three directions (LD, TD, ST), shear, plane strain tests and R_{LD} value for 5 plastic work levels and imposing $C_{44}=C_{55}=C_{66}$ (Table 2).

Table 2: Coefficients of CPB06 yield function for TA6V for 5 plastic works leves (*a=2*)

W_p	k	C_{11}	C_{12}	C_{13}	C_{22}	C_{23}	C_{33}	C_{66}
1.857	-0.136	1	-2.373	-2.364	-1.838	1.196	-2.444	3.607
9.377	-0.136	1	-2.495	-2.928	-2.283	1.284	-2.446	4.015
48.66	-0.165	1	-2.428	-2.920	1.652	-2.236	1.003	-3.996
100.2	-0.164	1	-2.573	-2.875	1.388	-2.385	0.882	-3.926
206.6	-0.180	1	-2.973	-2.927	0.534	-2.963	0.436	-3.883

Numerical results of the CPB06 constitutive model are compared with the corresponding experimental observations and shown in Figs. 5, 6 and 7. The corresponding theoretical yield surfaces along with the experimental values (symbols) for 5 levels of plastic work are shown in Fig. 5. Three biaxial plane projections of the yield loci are shown (LD-TD, LD-ST and TD-ST) as well as the π-plane projection. Note that irrespective of the level of plastic work, the yield loci have a distorted elliptical shape. In this figure, it is clearly demonstrated that the

correlations, for each loading direction and strain path, are in good agreement with the experimental observations.

With the purpose of observing the plastic anisotropy predictions of CPB06 model, strain field predictions of compression tests in LD, TD and ST directions were also compared with experimental results (Fig. 6). The results show that both values and shape of the strain distribution are well predicted but with slightly higher error in ST direction.

Finally, Fig. 7 shows the experimental stress-strain curves along with the model correlation. It can be seen that except for compression in the TD direction, the stress strain response is successfully correlated. It is worth noting that the different curves for both tension and compression in three directions (LD, TD, ST), confirm that von Mises isotropic approach is insufficient to describe the mechanical behaviour of TA6V titanium alloy.

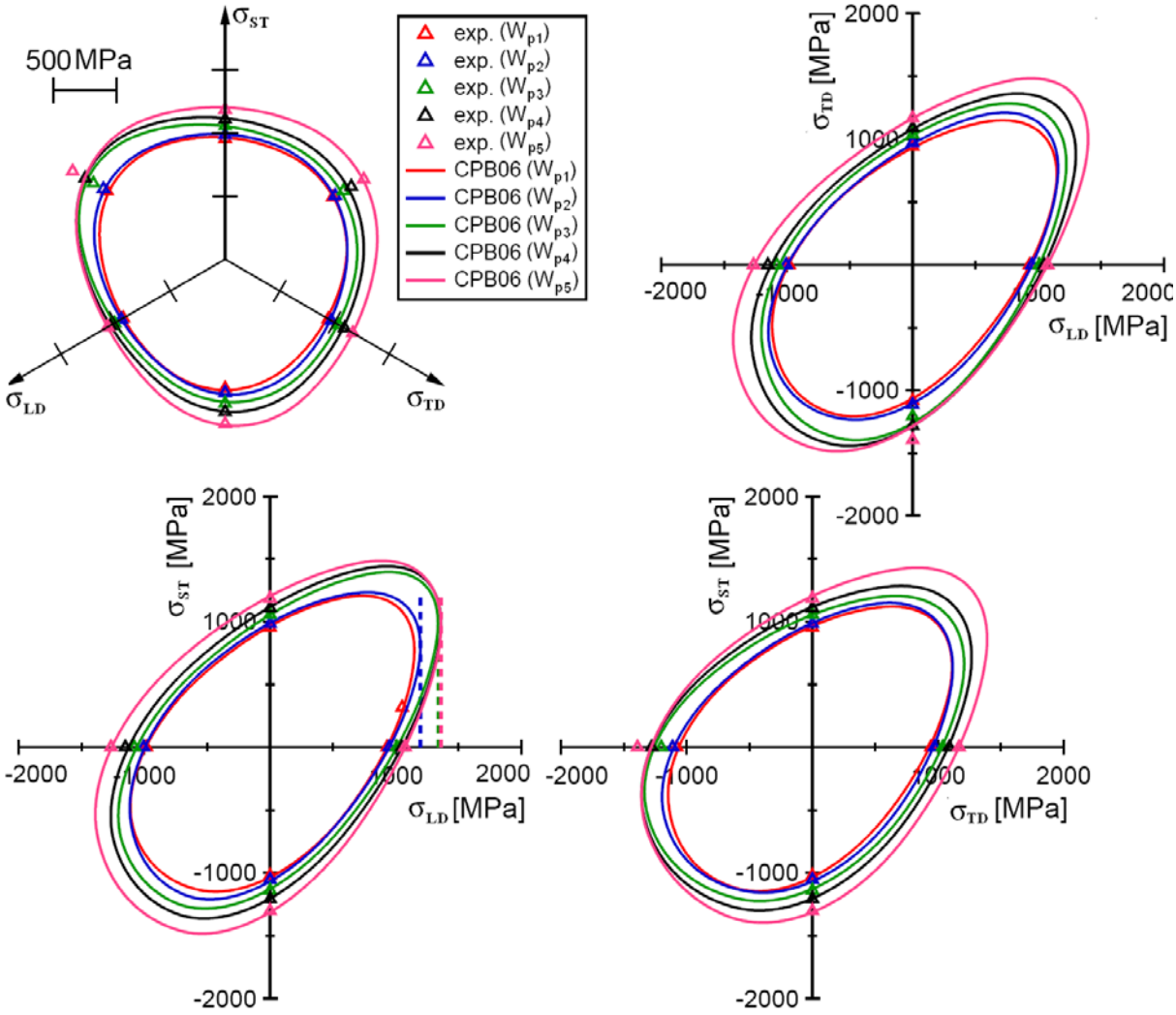

Figure 5: Yield loci predicted by CPB06 and experimental points for 5 accumulated plastic works: W_{p1}= 1.86, W_{p2}=9.38, W_{p3}=48.7, W_{p4}=100.2 and W_{p5}=206.6 J/cm^3.

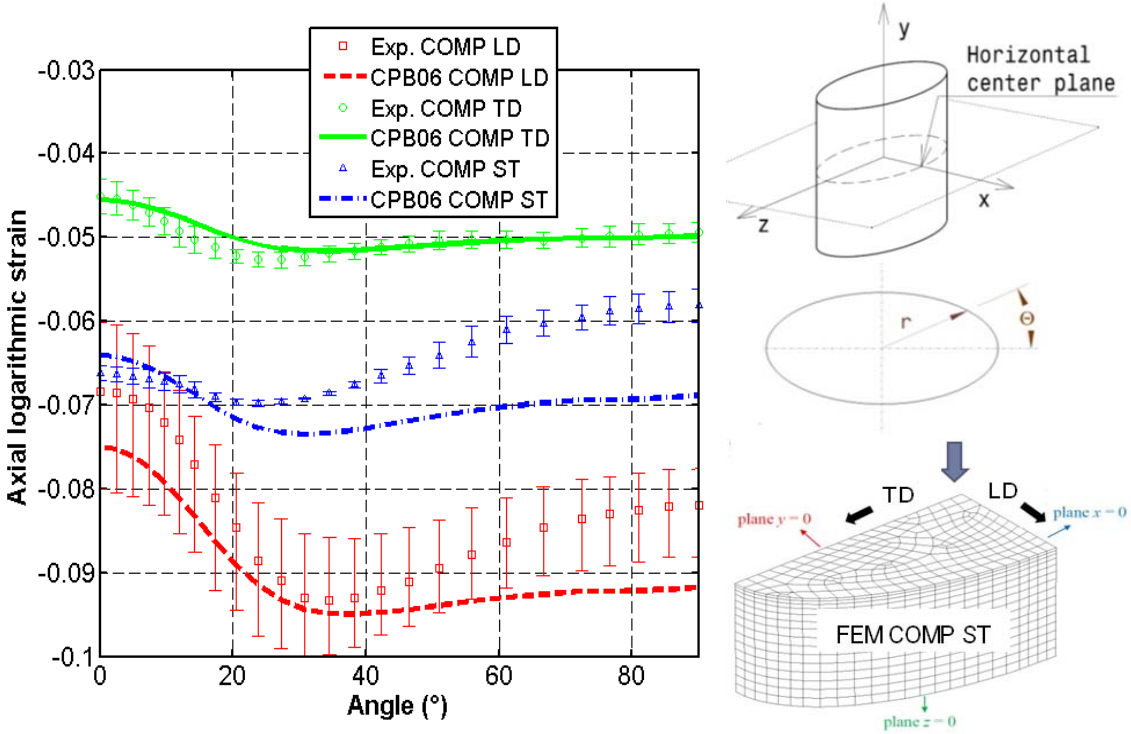

Figure 6: Experimental (DIC) and CPB06 predictions of axial strain distribution along the surface of the median cross-section of compression samples for LD at ε_{axial}=0.08%, TD at ε_{axial}=0.05% and ST at ε_{axial}=0.065%.

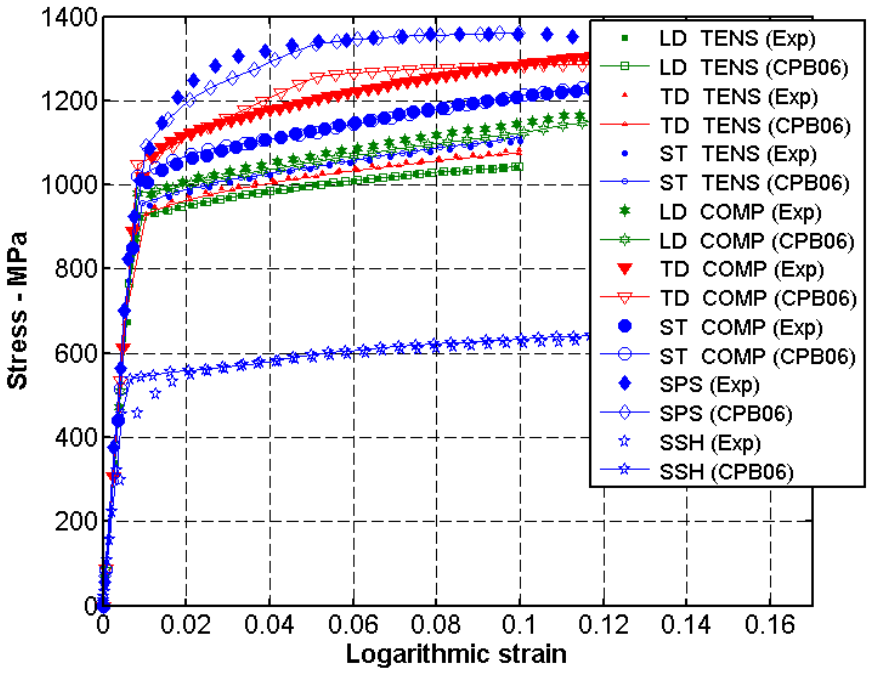

Figure 7: Experimental and CPB06 predictions of stress-strain curves in tension (TENS) and compression (COMP) for LD, TD and ST directions, plane strain LD-ST (SPS) and shear (SPS) LD-ST (10^{-3} s^{-1} and RT).

4 VALIDATION OF THE MODEL APPROACH

Tensile test on a notched specimen generating an initial maximum triaxiality of 1.2 is used in order to evaluate the identified CPB06 model (Fig. 8).

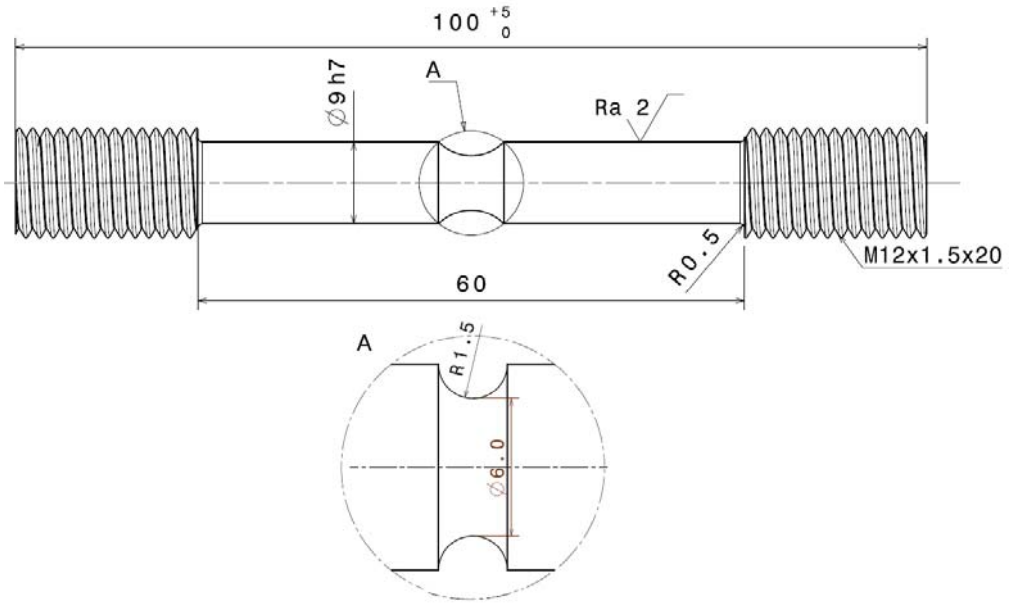

Figure 8: Geometry of the sample for notch tensile tests.

The experimental cross-section of the geometry just before rupture and the load as a function of the displacement for a 40mm gauge zone are compared with predictions of CPB06 based on 4 different material parameter input identified with different set of experimental tests data:

1. Initial CPB06 yield locus identified with compression and tension tests for LD, TD and ST with Voce type hardening law
2. Initial CPB06 yield locus identified with compression and tension tests for LD, TD and ST, shear and plane strain tests with Voce type hardening law
3. CPB06 identified with compression and tension tests for LD, TD and ST, shear, plane strain tests and $R_{LD}=1.15$ value for 5 plastic work levels
4. CPB06 identified with compression and tension tests for LD, TD and ST, shear, plane strain tests and $R_{LD}=1.15$ value for 5 plastic work levels and imposing $C_{44}=C_{55}=C_{66}$ (data set used for Fig. 5 to 7).

Results show that identification done with the highest number of monotonic tests fits better both, the load prediction and the shape of the deformed cross-section of the sample. However, the constraint of $C_{44}=C_{55}=C_{66}$ is needed in order to assure the correct load prediction of the CPB06 model.

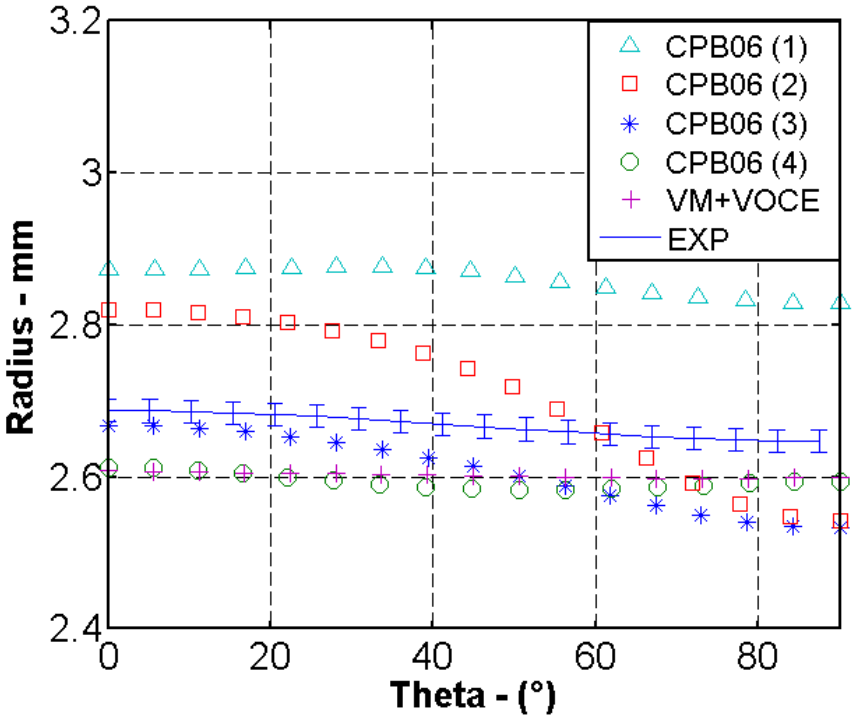

Figure 9: CPB06 predictions of the cross-section of the notched specimen just before rupture.

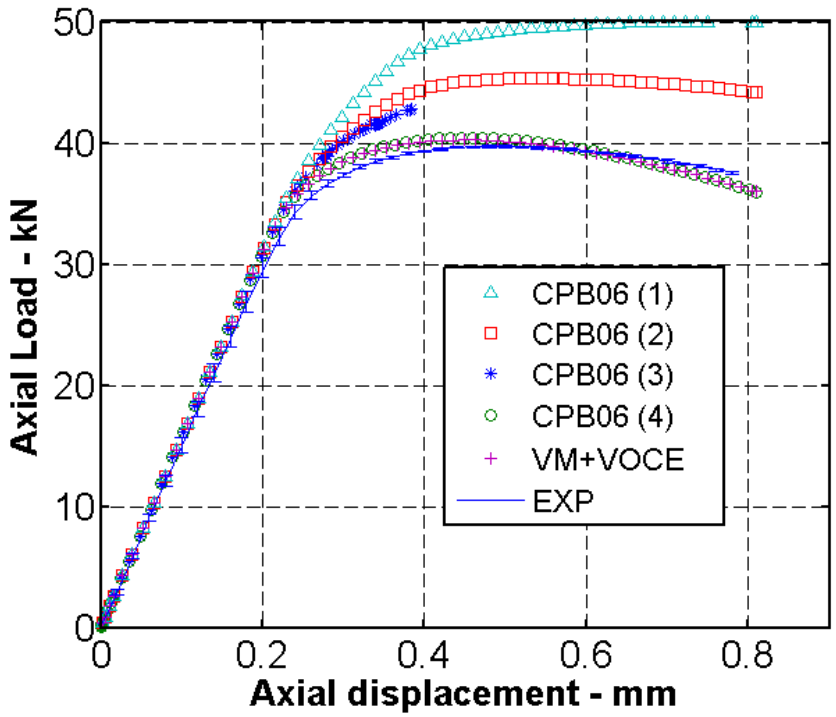

Figure 10: CPB06 predictions of the load vs. displacement for the notched specimen (40mm gauge length).

5 CONCLUSIONS

In the present work, the mechanical response of TA6V was studied with a set of tests at room temperatures and one strain rate of 10^{-3} s^{-1}. Yield stress anisotropy was observed and tension/compression tests have revealed that the material response is non-symmetric. On the basis of the available data, it can be concluded that the anisotropy in compression is more pronounced than in tension. Furthermore, experimental data was used in order to obtain material parameters of CPB06 criterion. The validity of the model was studied at quasi-static strain rate and room temperature. This model captures all the features of the observed behavior in monotonic tests (stress strain curves) and multiaxial stress strain tests (load, shape and strain distribution). The identification can still be improved in order to capture both load and shape predictions (or strain distribution) of a notched tensile tests.

For the future research there are three directions. First, Bauschinger effect on TA6V was not studied in this work. Second, the temperature and strain rate response need to be further identified. Lastly, analysis of damage by using notch tensile test with several triaxialities should be carried out in order to validate damage (FE) models.

REFERENCES

[1] Cazacu, O., Plunkett, B., Barlat, F. Orthotropic yield criterion for hexagonal close packed metals. *Int. J. Plasticity* (2006) **22**:1171-1194.

[2] Odenberger, E.L., Hertzman, J., Thilderkvist, P., Merklein, M., Kuppert, A., Stöhr, T., Lechler, J., Oldenburg, M. Thermo-mechanical sheet metal forming of aero engine components in Ti-6Al-4V – PART 1: Material characterisation. *Int. J. Mater. Form* (2012):1-12.

[3] Gilles, G., Hammami, W., Libertiaux, V. Cazacu, O. Yoon, J.H., Kuwabara, T., Habraken, A.M., Duchêne, L. Experimental characterization and elasto-plastic modeling of the quasi-static mechanical response of TA–6 V at room temperature. *Int. J. Solids Struct.* (2011) **48**:1277–1289.

[4] Tuninetti, V., Gilles, G., Milis, O., Lecarme, L., Habraken, A.M. Compression test for plastic anisotropy characterization using optical full-field displacement measurement technique. *Steel Res. Int.* SE: 14th Int'l Conf. Metal Forming 2012:1239-1242.

[5] Hammami, W., Tirry, W., Coghe, F., Duchene, L., Delannay, L., Habraken, A.M., Ti6A14V anisotropy and texture evolution predictions using Multisite and self consistent crystal plasticity models. *The 12th World Conference on Titanium Ti-2011* (2011).

[6] Majorell, A., Srivatsa, S. Picu, R.C. Mechanical behavior of TA6V at high and moderate temperatures – Part I: Experimental results. *Mater. Sci. Eng. A* (2002) **326(2):**297-305.

[7] Lee, W.S., Lin, C.F. Plastic deformation and fracture behaviour of TA6V alloy loaded with high strain rate under various temperatures. *Mater. Sci. Eng. A* (1998) **241(1–2)**:48-59.

[8] Plunkett, B. Cazacu, O., Barlat, F. Orthotropic yield criteria for description of the anisotropy in tension and compression of sheet metals. *Int. J. Plasticity* (2008) **24(5)**:847-866.

[9] Tuninetti, V., Gilles, G., Péron-Lührs, V. Habraken, A.M. Compression Test for Metal Characterization using Digital Image Correlation and Inverse Modeling, *Procedia IUTAM* (2012) **4:**206-214

[10] Khan, A.S., Suh, Y.S., Kazmi, R. Quasi-static and dynamic loading responses and

constitutive modeling of titanium alloys. *Int. J. Plasticity* (2004) **20:**2233–2248.
[11] Flores, P. Development of Experimental Equipment and Identification Procedures for Sheet Metal Constitutive Laws. Ph.D. Thesis (2005). University of Liège,.
[12] Flores, P., Tuninetti, V., Gilles, G., Gonry, P., Duchêne, L., Habraken, A.M. Accurate stress computation in plane strain tensile tests for sheet metal using experimental data. *J. Mater. Process. Technol.* (2010) **210(13)**:1772-1779.
[13] Lou, X.Y., Li, M., Boger, R.K., Agnew, S.R., Wagoner, R.H. Hardening evolution of AZ31B Mg sheet. *Int. J. Plasticity* (2007) **23**:44-86.
[14] Plunkett, B., Cazacu, O., Lebensohn, R.A., Barlat, F. Evolving yield function of hexagonal materials taking into account texture development and anisotropic hardening. *Acta Mater.* (2006) **54**:4159-4169.
[15] Hastings, W.K. Monte Carlo sampling methods using Markov chains and their applications. *Biometrika* (1970) **57**:97-109
[16] Metropolis, N., Rosenbluth, A.W., Rosenbluth, M.N., Teller, A.H., Teller, E. Equation of state calculations by fast computing machines. *J. chem. Phys* (1953) **21**:1087-1092.

ACKNOWLEDGEMENTS

The authors thank the Walloon Region, the Belgian Scientific Research Fund FNRS which finances A.M.H. and the Interuniversity Attraction Poles Program, Belgian Science Policy P7/21 Intemate, for financial support.